Nanoindentation Induced Deformation Near Grain Boundaries of Corrosion Resistant Nickel Alloys

F. William Herbert[1], Bilge Yildiz[2] and Krystyn J. Van Vliet[1]
[1]Department of Materials Science & Engineering, Massachusetts Institute of Technology, 77 Mass. Av., Cambridge, MA 02139
[2] Department of Nuclear Science & Engineering, Massachusetts Institute of Technology, 77 Mass. Av., Cambridge, MA 02139

ABSTRACT

The damage accumulation behavior of different grain boundary structures in Inconel 690 (Ni-29wt%Cr-9wt%Fe) was investigated in the presence of large, localized plastic strains induced by nanoindentation. Spatially-resolved hardness was measured as a function of lateral distance from 'random' high-angle grain boundaries and twin boundaries. The confinement of induced defects between the indenter tip and grain boundaries did not lead to significant differences in measured hardness between high angle and twin boundaries. Critical "pop-in" loads indicating the onset of incipient plasticity were lower within 1μm of grain boundaries, but were statistically equivalent for random and twin boundaries. These results suggest a comparable extent of dislocation mobility and absorption at the different grain boundary types in Inconel 690 under ambient conditions.

INTRODUCTION

Grain boundaries are regions of crystalline incompatibility during plastic flow where dislocations may originate [1] and/or accumulate [2] during shear. Grain boundary engineering to increase the fraction of "special", low-energy boundaries -has been shown to improve resistance to creep [3], fracture [4], embrittlement and corrosion [5]. The response of twin (CSL Σ3) and 'random' high-angle grain boundaries to localized plastic strains is therefore likely to vary significantly. Understanding this nanoscopic behavior subsequently provides insight into the chemomechanical origins of complex degradation mechanisms such as inter-granular stress corrosion cracking. Previous nanoindentation experiments have variably suggested that local hardness: is raised by 10-15% within 1μm either side of grain boundaries in BCC alloys [6], is raised by ~20% on grain boundaries with a corresponding reduction in critical pop-in loads required to nucleate dislocations in Fe [7], either increases by 50% or decreases slightly within 2μm near grain boundaries in Cu [8], and remains statistically homogeneous across grain boundary regions in Ni_3Al [9]. Although grain boundary types were reported in these studies, a clear picture of the misorientation effect on damage accumulation behavior has not emerged. This study focused on the boundary character influence on both nanohardness and critical loads for incipient plasticity in the vicinity of different grain boundaries in the nickel-based alloy Inconel 690.

EXPERIMENTAL

A polycrystalline sample of Inconel 690 alloy (Ni-29wt%Cr-9wt%Fe) was annealed at 1107°C for 15 minutes and water quenched to produce a grain size of roughly 60μm with a wide variety of grain orientations. The sample was mechanically polished with a final suspension of 0.05μm colloidal silica. Transmission electron microscopy showed that impurity and second phase particle segregation at grain boundaries was negligible in this sample (data not shown). Instrumented nanoindentation was conducted using a Hysitron TriboIndenter employing a diamond Berkovich (trigonal pyramid) tip. Grain boundaries were imaged by using the indenter as a scanning probe and nanoindentations were placed in diagonal lines running across each grain boundary (Fig. 1) according to the method developed by Soer et al [6]. Indentations were made in load control to a depth of ~ 200nm, with inter-indentation spacing of >2μm to minimize interaction between neighboring indentation volumes. Hardness data were extracted using the Oliver-Pharr method [10] from the initial 40% of the unloading portion of the nanoindentation load-displacement responses. The grain boundary types were subsequently characterized by electron backscatter diffraction in a Zeiss Supra55 SEM using EDAX software. The boundaries were classified into three groups: low angle boundaries (<15% misorientation), special (Σ3 twins and higher-order variants) and random high-angle boundaries (all other misorientations >15%).
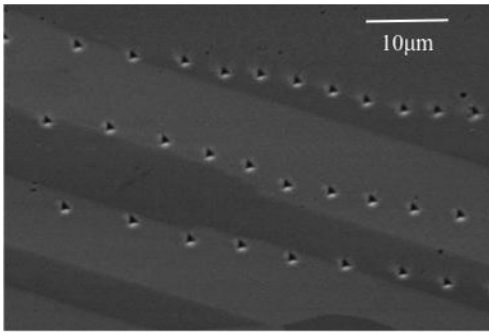

Figure 1. Indentations were located at varying distances from grain boundaries (indicated here as boundaries between regions of darker and lighter contrast).

RESULTS AND DISCUSSION

We systematically assessed the hardness, the dependence of hardness on distance-to-grain boundary, and the critical loads p_c for incipient "pop-ins" in the indentation load-displacement data as measures of different responses of grain boundaries to indentation-induced plasticity.

Nanohardness in the vicinity of grain boundaries

Results were obtained from fifteen different Σ3 (60° misorientation) twin boundaries and eleven high-angle boundaries, with over 300 discrete nanohardness readings for each boundary type. Typical examples in Figure 2 illustrate two distinct hardening responses shown by individual grain boundaries as a function of boundary-to-indenter tip distance. In Figure 2(a) the nanohardness increased within 4μm of a twin boundary on average by 9% over the grain centre. This type of increase was observed for six out of the fifteen twin boundaries studied. For the other nine, as in Figure 2(b), no hardening trend was discernable. Likewise, 4/11 random boundaries gave an average 9% hardness increase for indentations within ~3μm of the boundary while the remainder produced no particular trend, shown in Figures 2(c) and (d) respectively.
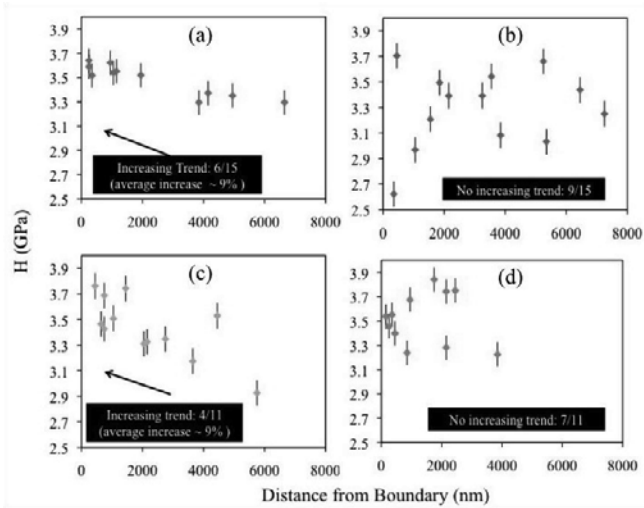

Figure 2. Representative hardness values resulting from indentations described in Fig.1, from 15 different twin boundaries in (a) and (b); and 11 random grain boundaries in (c) and (d). In both cases, fewer than half of tested boundaries produced a recognizable rising trend in hardness adjacent to the boundary.

Figure 3 shows the natural logarithm of hardness as a function of distance from these two generic grain boundary types. Data were selected only from those boundaries that gave a visible rising trend in hardness with decreasing distance (as in Figures 2(a) and (c)). The data are fit to a Hall-Petch type empirical relationship (Eq.1) in the context of grain boundary strengthening mechanisms [2,11,12].

$$H = H_o + k.d^{-n}$$ (1)

where H is hardness, H_o an intrinsic material constant, k and n are grain boundary strengthening parameters and d is a characteristic length scale taken as the indent-boundary distance here.
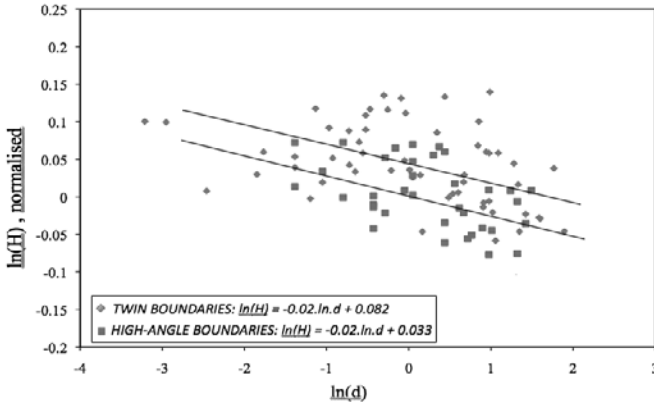
Figure 3. Hardness, normalized by average hardness for each grain centre, as a function of distance from the grain boundary in a "Hall-Petch" type plot. The upper line is the best-fit linear regression for the twin boundaries, with a slope of -0.02; the lower line is for the high angle grain boundaries with identical slope -0.02.

The gradient of these trends for high angle and twin grain boundaries in Figure 3 is equivalent, indicating that the strengthening parameter n in Eq.1 is the same for both boundary types (equal to -0.02). This suggests the mechanism of damage accumulation, or the nature of the interaction between induced dislocations with the planar defects, is either identical for twin and high angle boundaries at room temperature, or cannot be distinguished using this technique. Nevertheless, the intercept of these lines differs and on average twin boundaries showed higher hardness in their vicinity. One interpretation of the increased intercept for ln(H) is the other strengthening parameter k may be larger for the twin boundaries (Eqs. 2 and 3). However, given the scattered nature of the data, we cannot confidently assert that the discrepancy in the factor k is fundamentally related to differences between grain boundary types.

$$\ln\left(\frac{k_{TWIN}}{k_{HAB}}\right) = 2.48 \tag{2}$$

$$\frac{k_{TWIN}}{k_{HAB}} = 11.94 \tag{3}$$

Incipient plasticity

The critical loads p_c for incipient "pop-ins" - discontinuous bursts related to the sudden motion of dislocations [8] – were measured by noting on the nanoindentation load-displacement curves the first displacement increase larger than 5nm at constant load. Pop-in loads were compared for indentations within 1μm of high-angle grain boundaries and twin boundaries and indentations made "far"(> 5μm) from the boundaries (Figure 4).
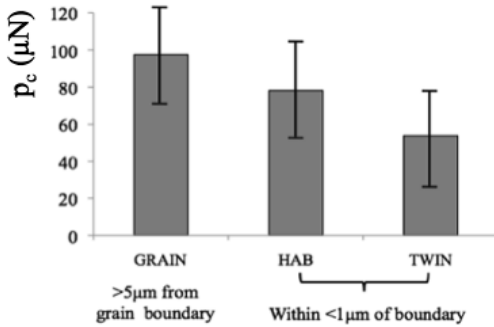
Figure 4. Critical pop-in load for indentations "far" from boundaries (grain), and within 1μm of high-angle grain boundaries (HAB) and twin boundaries (TWIN).

A reduction in p_c was observed for indentations placed adjacent to both high-angle and twin boundaries. A grain boundary may act as a primary source of dislocations during deformation [8], facilitating plastic yield at lower loads. While twin boundaries seem to promote incipient plasticity at lower applied loads, the range of error overlaps between the twin- and high angle boundary data, and also with grain center values. Hence we cannot report unequivocally that the observed p_c reduction is a purely misorientation-related phenomenon.

CONCLUSIONS

The effect of grain boundary character on the mechanical response to spatially-resolved nanoindentation was systematically investigated in Inconel 690. Approximately 40% of grain boundaries displayed a discernable rising trend in nanohardness within 3-4μm of their vicinity. The average rise in nanohardness was 9%, regardless of the grain boundary type. An analogue of the grain boundary strengthening (Hall-Petch) relationship suggested that high symmetry twin boundaries produced a stronger hardening response as compared to randomly-oriented high angle boundaries. However these results do not elucidate the nature of dislocation interaction mechanisms for different grain boundary types under severe, localized damage. Further, the critical load at which yielding first

occurs is smaller in the vicinity of grain boundaries, suggesting that these act as dislocation sources in the incipient stages of plasticity. We note that these nanoindentation measurements were conducted at room temperature, wherein the dislocation mobility and absorption may be comparably small for both types of boundaries.

REFERENCES

[1] E.V. Esquivel, L.E. Murr, *Materials Science & Engineering A* 409 (2005)

[2] M.F. Ashby, *Philosophical Magazine* 21 (1970)

[3] V. Thaveepringsriporn, G.S. Was, *Metall. Trans.* 28A: 2101 (1997)

[4] J. Marrow, D. Engelberg, A. Jivkov, P. Wood, L. Babout, N Stevens, *Energy Materials* 1(2) (2006)

[5] V. Randle, *Mat. Sci. & Technology* 26(3) (2010)

[6] W.A. Soer, K.E. Aifantis, J. ThM DeHosson*, Acta Materialia* 53 (2005)

[7] Ya.M. Soifer, A. Verdyan, M. Kazakevich, E. Rabkin, *Scripta Materialia* 47 (2002)

[8] T. Ohmura, K. Tsuzaki, *J. Phys. D: Appl. Phys* 41 (2008)

[9] P.C. Wo, A.H.W. Ngan, *J. Materials Research Society* 19(1) (2004)

[10] A.C. Fisher-Cripps, *Nanoindentation,* Springer 2nd Ed. (2004)

[11] N.J. Petch, *J. of the Iron & Steel Institute* 6(1) (1953)

[12] E.V. Esquivel, L.E. Murr, *Materials Science & Engineering A* 409 (2005)